

Multiple currents in charged beams

D.A. Burton, J. Gratus, and R.W. Tucker
Department of Physics, Lancaster University, UK
& The Cockcroft Institute, UK
(Dated: April 2, 2019)

It is argued that continuum realisations of distributions of collisionless charged particles should accommodate a dynamically evolving number of electric currents even if the continuum is composed of only one species of particle, such as electrons. A model is proposed that self-consistently describes the interaction of such a continuum and its electromagnetic field. It is formulated using a Lagrangian approach and employs a “folded” flow map to describe the bulk particle motion. An asymptotic perturbation scheme is developed to analyse ultra-relativistic multi-component current configurations. The model is fully relativistic and is formulated over Minkowski spacetime using intrinsic tensor field theory.

PACS numbers: 41.75.Ht, 29.27.-a, 52.59.Dk, 52.27.Jt

I. INTRODUCTION

Progress in high-energy physics relies on accelerator designers contemplating charged particle beams of ever higher energies and intensities. As schemes for accelerating charged particles become more complex and ambitious in their aims, it is apparent that some existing theoretical models are inadequate for a proper understanding of new challenges. In many existing models, matter is represented using classical point particles and it is not clear how to unambiguously and consistently model their electromagnetic interaction.

The nub of the problem is precisely how one should sensibly formulate the interaction of a classical point charge with its *own electromagnetic field*. The charge density of a point particle is singular and must therefore be handled carefully. Assumptions must be made about how the singular Coulombic stresses are compensated by non-electromagnetic stresses when calculating the particle’s self-force. This issue was addressed by Dirac [1] nearly 70 years ago and led to the covariant Lorentz-Dirac equation for the trajectory of a point charge in an external electromagnetic field. However, unlike more familiar equations of particle mechanics, the Lorentz-Dirac equation is a *third-order* ordinary differential equation in proper time for the particle’s trajectory and has a number of unusual properties including self-acceleration and pre-acceleration. Unless special final conditions are adopted, it predicts that an isolated and free point charge with non-zero initial velocity will accelerate forever and if the particle is subjected to a sharp electromagnetic pulse it will begin to move before the pulse reaches it. Methods for evading such unpalatable conclusions involve iterating the Lorentz-Dirac equation in powers of its charge q_0 . Landau and Lifshitz [2] showed that truncating the resulting series to any *finite* order leads to a second-order evolution equation yielding particle trajectories with more reasonable properties. Although their argument yields a workable scheme, it is not at all clear that it may be generalised to a collection of accelerating high-energy charged particles in close proximity. Neglect-

ing higher-order terms in q_0 may be suspect when the particle number density is sufficiently high. In conclusion, a number of ad-hoc choices must be made to obtain a sensible relativistic equation of motion for a collection of charged point particles starting from first principles. For a recent account of the issues concerning the derivation of the Lorentz-Dirac equation see [3].

Many of the above issues are due to the uneasy marriage of field and point particle concepts in classical electrodynamics. Classical point particles are a convenient idealisation and one might argue that quantum theory must be invoked to yield a palatable answer. However, the testy relationship between fields and point particles resurfaces in quantum electrodynamics where divergences in “bare” quantities must be regulated prior to renormalisation to obtain physical results.

Given the above complexities and reservations, an alternative approach has recently been developed [3] to analyse the ultra-relativistic dynamics of a collection of accelerating charged particles. The attitude adopted in [3] and the present article is that models of matter based on classical relativistic field theory are more suitable for high-energy beam dynamics than those employing classical point particle notions. The model in [3] employs a smooth relativistic field description of the electromagnetic *and* matter content where the total energy and momentum of the electromagnetic and matter fields are conserved. Charged matter is modelled as a 4-vector field on spacetime whose trajectories describe the bulk particle motion.

The partial differential equations governing the electromagnetic and matter fields in this article are fully coupled and non-linear. Although exact solutions describing highly symmetric configurations can be found, the system of equations is in general only tractable when subjected to an approximation scheme. Such a scheme, based on a covariant asymptotic expansion in a running parameter $\varepsilon > 0$ around the light-cone, was introduced in [3] and permits calculation of the detailed dynamics of ultra-relativistic charged particle beams in external electromagnetic fields. In principle, one can calculate the

field quantities to any desired finite order in ε .

The present article focuses on some of the issues encountered when analysing the model in [3]. Specifically, the non-linearities in the field equations may lead to solutions whose charge density diverges despite being initially regular. Sections II and III briefly review the charged continuum model in [3] and show that diverging solutions exist satisfying a substantial range of initial conditions. This behaviour is commonplace in many continuum models in physics, such as in neutral gas dynamics and fluid dynamics, and is often ameliorated by including dissipative processes. Section IV argues that dissipative processes will not prevent the formation of multiple currents in charged beams. Sections V and VI develop and analyse a continuum model accommodating currents with a dynamical number of components and section VII extends the ultra-relativistic analysis methods introduced in [3] to multi-component charged currents.

II. SINGLE CURRENT CHARGED CONTINUA

The model discussed in this section and in [3] describes a collection of accelerating charged particles, with (rest) mass m_0 and charge q_0 , as a dynamical continuum. The vector field V is the 4-velocity of the continuum on space-time and its integral curves describe the bulk motion of the collection of charged particles. The scalar field \mathcal{N} is the particle number density measured by a comoving observer and $\rho = \frac{q_0^2}{\epsilon_0 m_0 c^2} \mathcal{N}$ is called the *reduced* proper charge density where ϵ_0 is the permittivity of the vacuum and c is the speed of light in the vacuum. In what follows, units are chosen in which $c = 1$.

The antisymmetric rank 2 covariant tensor field F (a 2-form) encodes the electromagnetic field and the triple (V, ρ, F) satisfies the covariant Maxwell equations [4]

$$dF = 0, \quad (1)$$

$$d \star F = -\rho \star \tilde{V}, \quad (2)$$

on Minkowski spacetime (\mathcal{M}_4, g) where g is the metric tensor. In an inertial Cartesian coordinate system (t, x, y, z) in the laboratory frame

$$g = -dt \otimes dt + dx \otimes dx + dy \otimes dy + dz \otimes dz,$$

d is the exterior derivative, \star is the Hodge map associated with g and the 1-form \tilde{V} is defined by the property $\tilde{V}(X) = g(V, X)$ for any vector field X . The field equations for V are obtained using energy-momentum conservation $d\tau_K = 0$ where the total stress-energy-momentum 3-form τ_K is the sum of matter and electromagnetic contributions :

$$\tau_K = \rho g(V, K) \star \tilde{V} + \frac{1}{2} (i_K F \wedge \star F - F \wedge i_K \star F)$$

and the vector field K is a spacetime translation on \mathcal{M}_4 . Setting K to ∂_t , ∂_x , ∂_y and ∂_z in $d\tau_K = 0$ yields the ∂_t ,

∂_x , ∂_y and ∂_z components of the equation

$$\nabla_V \tilde{V} = i_V F, \quad (3)$$

where

$$g(V, V) = -1 \quad (4)$$

with ∇ the Levi-Civita connection on \mathcal{M}_4 and i_V the interior (contraction) operator on forms. The term $i_V F$ in (3) is a continuum generalisation of the covariant expression for the Lorentz force on a point charge (the charge to mass ratio q_0/m_0 has been absorbed into the definitions of ρ and F) where the tangent to the point charge's proper-time parametrised worldline has been replaced by V . The charged matter drives the electromagnetic field through (2) and the electromagnetic field acts back on the matter through (3) conserving total energy and momentum.

Equations (1-4) are well-known in charged plasma physics and are often said to describe a “cold charged fluid”. They have found application to accelerator physics [5] in recent years and have proved useful for examining the stability of high intensity particle beams.

III. DEVELOPMENT OF SINGULARITIES IN THE CHARGE DENSITY

In [3] highly symmetric exact solutions to (1-4) describing “walls of charge” were used to motivate a hierarchy of field equations for modelling ultra-relativistic charged particle beams. Exact solutions to (1-4) of the form

$$F = \mathcal{E}(t, z) dt \wedge dz, \\ V = \frac{1}{\sqrt{1 - \mu^2(t, z)}} (\partial_t + \mu(t, z) \partial_z) \quad (5)$$

were sought, where $\mu \partial_z$ is the Newtonian velocity of the charge distribution as measured by the laboratory observer ∂_t . Using (1-5) it follows that

$$d\mathcal{E} = \rho \# \tilde{V}, \quad (6)$$

$$\bar{\nabla}_V \tilde{V} = \mathcal{E} \# \tilde{V}, \quad (7)$$

$$\bar{g}(V, V) = -1 \quad (8)$$

where the projected metric \bar{g} is

$$\bar{g} = -dt \otimes dt + dz \otimes dz,$$

$\#$ is the Hodge map associated with the volume 2-form $\#1 \equiv dt \wedge dz$, $\bar{\nabla}$ is the Levi-Civita connection of \bar{g} and $\tilde{V}(X) = \bar{g}(V, X)$ for any vector X on 2-dimensional Minkowski spacetime \mathcal{M}_2 with metric \bar{g} . Equation (6) implies

$$V \mathcal{E} = 0 \quad (9)$$

i.e. the electric field is constant along the integral curves of V and so, using (7), the magnitude of the acceleration

$\bar{\nabla}_V V$ is constant along the integral curves of V . Therefore, the continuum undergoes local hyperbolic motion and it is straightforward to solve to (6-8) in a comoving coordinate system (τ, σ) adapted to V , as shown in [3], where $V = \partial_\tau$ and $z = \sigma$ on the initial hypersurface $\tau = 0$. For charge distributions initially at rest the Jacobian of the transformation between (τ, σ) and (t, z) is non-degenerate for all τ and σ [3]. Using (6) it follows that, for all $\tau > 0$, ρ is well-behaved for charge distributions at rest at $\tau = 0$.

The purpose of this section is to demonstrate that more general initial conditions lead to divergences in the reduced proper charge density ρ over finite time. In [3] particular examples of ρ were generated using expressions for V and \mathcal{E} as functions of $\tau = \hat{\tau}(t, z)$ and $\sigma = \hat{\sigma}(t, z)$. For the present purposes it is more convenient to formulate an ordinary differential equation for ρ along V and examine properties of its solutions. The integrability condition

$$d(\rho \# \tilde{V}) = 0$$

following from (6) is written

$$V\rho = -\rho\theta \quad (10)$$

where the scalar $\theta \equiv \#^{-1}d\#\tilde{V}$ is the divergence of V . Equations (10), (9) and $V\theta = f(\rho, \theta, \mathcal{E})$ for some f forms a closed first-order ordinary differential system for $(\rho, \theta, \mathcal{E})$ along the integral curves of V . An explicit expression for f is obtained below.

Using the identity (see, for example, page 229 of [4])

$$(\mathcal{L}_V \bar{g})(X, Y) = \bar{g}(X, \bar{\nabla}_Y V) + \bar{g}(Y, \bar{\nabla}_X V) \quad (11)$$

where X and Y are any vector fields on \mathcal{M}_2 and \mathcal{L}_V is the Lie derivative with respect to V , it follows that

$$\begin{aligned} (\mathcal{L}_V \tilde{V})(X) &= (\mathcal{L}_V \bar{g})(V, X) \\ &= \bar{g}(V, \bar{\nabla}_X V) + \bar{g}(X, \bar{\nabla}_V V) \end{aligned} \quad (12)$$

and, using (8),

$$\begin{aligned} \bar{g}(V, \bar{\nabla}_X V) &= \frac{1}{2} \bar{\nabla}_X (\bar{g}(V, V)) \\ &= 0, \end{aligned} \quad (13)$$

since $\bar{\nabla}$ is metric-compatible. Therefore, (12) yields

$$\mathcal{L}_V \tilde{V} = \bar{\nabla}_V \tilde{V}. \quad (14)$$

Using Cartan's identity [4] $\mathcal{L}_V = i_V d + d i_V$ on forms it follows

$$\mathcal{L}_V \tilde{V} = i_V d\tilde{V} \quad (15)$$

and so the following expressions for the relativistic acceleration $\mathcal{A} \equiv \bar{\nabla}_V V$ of V are obtained:

$$\tilde{\mathcal{A}} = \bar{\nabla}_V \tilde{V} = i_V d\tilde{V} = \mathcal{E} \# \tilde{V} \quad (16)$$

where (7), (14) and (15) have been used and $\tilde{\mathcal{A}}(X) = \bar{g}(\mathcal{A}, X)$ for any vector X on \mathcal{M}_2 . Since there are no 3-forms on 2-dimensional manifolds $\tilde{V} \wedge d\tilde{V} = 0$ and

$$\begin{aligned} i_V(\tilde{V} \wedge d\tilde{V}) &= 0 \\ &= (i_V \tilde{V})d\tilde{V} - \tilde{V} \wedge i_V d\tilde{V}. \end{aligned} \quad (17)$$

Using (17), (16) and $i_V \tilde{V} = \bar{g}(V, V) = -1$, it follows that

$$d\tilde{V} = \mathcal{E} \# 1. \quad (18)$$

Any frame field (X_0, X_1) and its dual coframe field (e^0, e^1) on \mathcal{M}_2 satisfy

$$\begin{aligned} e^a(X_b) &= \delta_b^a, \\ \delta_b^a &\equiv \begin{cases} 1 & \text{if } a = b \\ 0 & \text{if } a \neq b \end{cases} \end{aligned} \quad (19)$$

where the indices a, b run over 0, 1. The intrinsic curvature of $\bar{\nabla}$ is zero so

$$\bar{\nabla}_V \bar{\nabla}_{X_a} V - \bar{\nabla}_{X_a} \bar{\nabla}_V V - \bar{\nabla}_{[V, X_a]} V = 0 \quad (20)$$

where $[V, X_a]$ is the Lie bracket of V and X_a . The divergence $\theta = \#^{-1}d\#\tilde{V}$ of V may be written [9]

$$\theta = \bar{\nabla} \cdot V = e^a(\bar{\nabla}_{X_a} V)$$

hence

$$\begin{aligned} V\theta &= \bar{\nabla}_V(\bar{\nabla} \cdot V) \\ &= (\bar{\nabla}_V e^a)(\bar{\nabla}_{X_a} V) + e^a(\bar{\nabla}_V \bar{\nabla}_{X_a} V) \\ &= (\bar{\nabla}_V e^a)(\bar{\nabla}_{X_a} V) + \bar{\nabla} \cdot \mathcal{A} + e^a(\bar{\nabla}_{[V, X_a]} V) \end{aligned} \quad (21)$$

where (20) and (16) have been used. The torsion of $\bar{\nabla}$ vanishes

$$\bar{\nabla}_V X_a - \bar{\nabla}_{X_a} V - [V, X_a] = 0$$

and so, using (19)

$$\begin{aligned} \bar{\nabla}_V e^a &= -\left(e^a(\bar{\nabla}_V X_b)\right) e^b \\ &= -\left(e^a(\bar{\nabla}_{X_b} V) + e^a([V, X_b])\right) e^b. \end{aligned} \quad (22)$$

Using (22) to eliminate $\bar{\nabla}_V e^a$ in (21) yields

$$V\theta = \bar{\nabla} \cdot \mathcal{A} - \text{tr}(\bar{\nabla} V \bar{\nabla} V) \quad (23)$$

where $\bar{\nabla} V = e^b(\bar{\nabla}_{X_a} V) e^a \otimes X_b$ and $\text{tr}(\bar{\nabla} V \bar{\nabla} V) = e^b(\bar{\nabla}_{X_a} V) e^a(\bar{\nabla}_{X_b} V)$. The scalar $\text{tr}(\bar{\nabla} V \bar{\nabla} V)$ is obtained using the following \bar{g} -orthonormal frame field $\{X_0, X_1\}$ adapted to V and its dual frame field $\{e^0, e^1\}$:

$$\begin{aligned} X_0 &= V, & X_1 &= \widetilde{\#} \tilde{V}, \\ e^0 &= -\tilde{V}, & e^1 &= \# \tilde{V} \end{aligned} \quad (24)$$

where the vector field $X_1 = \# \tilde{V}$ is defined by $\bar{g}(X, X_1) = (\# \tilde{V})(X)$ on any vector X on \mathcal{M}_2 . Using (13), (11) and (24) it follows that

$$\begin{aligned} \text{tr}(\bar{\nabla}V\bar{\nabla}V) &= (\bar{g}(X_1, \bar{\nabla}_{X_1}V))^2 \\ &= \frac{1}{4}((\mathcal{L}_V\bar{g})(X_1, X_1))^2 \end{aligned} \quad (25)$$

and expressing \bar{g} as

$$\begin{aligned} \bar{g} &= -e^0 \otimes e^0 + e^1 \otimes e^1 \\ &= -\tilde{V} \otimes \tilde{V} + \# \tilde{V} \otimes \# \tilde{V} \end{aligned}$$

it follows

$$\begin{aligned} \mathcal{L}_V\bar{g} &= -\mathcal{L}_V\tilde{V} \otimes \tilde{V} + \tilde{V} \otimes \mathcal{L}_V\tilde{V} \\ &\quad + \mathcal{L}_V\# \tilde{V} \otimes \# \tilde{V} + \# \tilde{V} \otimes \mathcal{L}_V\# \tilde{V} \end{aligned}$$

and

$$\begin{aligned} (\mathcal{L}_V\bar{g})(X_1, X_1) &= 2(\mathcal{L}_V\# \tilde{V})(X_1) \\ &= 2\theta \end{aligned} \quad (26)$$

where (19), (24), $\theta = \#^{-1}d\# \tilde{V}$ and Cartan's identity $\mathcal{L}_V = i_V d + d i_V$ on forms have been used. Equations (23), (26) and (25) give

$$V\theta = \bar{\nabla} \cdot \mathcal{A} - \theta^2 \quad (27)$$

and writing $\bar{\nabla} \cdot \mathcal{A}$ as a differential form yields

$$\begin{aligned} \bar{\nabla} \cdot \mathcal{A} &= \#^{-1}d\#\tilde{\mathcal{A}} \\ &= \#^{-1}d\#i_Vd\tilde{V} \\ &= -\#^{-1}d(\tilde{V} \wedge \#d\tilde{V}) \\ &= -\#^{-1}(d\tilde{V} \wedge \#d\tilde{V}) + \#^{-1}(\tilde{V} \wedge d\#d\tilde{V}). \end{aligned} \quad (28)$$

Thus, using (6), (18), and (28) it follows that (27) is

$$V\theta = \mathcal{E}^2 + \rho - \theta^2. \quad (29)$$

Equations (29), (10) and (9) are a closed system of differential equations for $(\rho, \theta, \mathcal{E})$ along V .

Let Γ be any proper-time parametrised integral curve of V :

$$\begin{aligned} \Gamma : I &\rightarrow \mathcal{M}_2, \\ \lambda &\rightarrow (t = T(\lambda), z = Z(\lambda)) \end{aligned}$$

where I is a subset of the real line \mathbb{R} and

$$\Gamma_*\partial_\lambda = V.$$

Hence, equations (9), (10) and (29) pulled back to \mathbb{R} using Γ^* are

$$\frac{d\mathcal{E}_\Gamma}{d\lambda} = 0, \quad (30)$$

$$\frac{d\rho_\Gamma}{d\lambda} = -\rho_\Gamma\theta_\Gamma, \quad (31)$$

$$\frac{d\theta_\Gamma}{d\lambda} = \mathcal{E}_\Gamma^2 + \rho_\Gamma - \theta_\Gamma^2 \quad (32)$$

where the subscript Γ indicates pull-back using Γ^* e.g. $\mathcal{E}_\Gamma(\lambda) = (\Gamma^*\mathcal{E})(\lambda) = \mathcal{E}(T(\lambda), Z(\lambda))$. The general solution to (31) is

$$\rho_\Gamma(\lambda) = \rho_0 \exp \left(- \int_0^\lambda \theta_\Gamma(\lambda') d\lambda' \right) \quad (33)$$

where $\rho_0 = \rho_\Gamma(0)$ is a value of ρ on an initial hypersurface. Since $\rho = \frac{q_0^2}{\epsilon_0 m_0 c^2} \mathcal{N}$ and the proper number density $\mathcal{N} \geq 0$ it follows $\rho_\Gamma \geq 0$. Over intervals of λ on which $d\rho_\Gamma/d\lambda \neq 0$ (30-32) yields

$$\begin{aligned} \frac{d\mathcal{E}_\Gamma}{d\rho_\Gamma} &= 0, \\ \frac{d\theta_\Gamma}{d\rho_\Gamma} &= \frac{1}{-\rho_\Gamma\theta_\Gamma}(\mathcal{E}_\Gamma^2 + \rho_\Gamma - \theta_\Gamma^2) \end{aligned}$$

and so

$$\rho_\Gamma^2 \frac{d}{d\rho_\Gamma}(\rho_\Gamma^{-2}\theta_\Gamma^2) = -\frac{2\mathcal{E}_\Gamma^2}{\rho_\Gamma} - 2$$

leading to the first integral

$$\theta_\Gamma^2 = \mathcal{E}_0^2 + 2\rho_\Gamma + \kappa_0\rho_\Gamma^2 \quad (34)$$

of (30-32) where κ_0 is a constant of integration determined by the initial values $\theta_\Gamma(0) = \theta_0$, $\rho_\Gamma(0) = \rho_0$ and $\mathcal{E}_\Gamma(0) = \mathcal{E}_0$.

According to (34) θ_Γ^2 is a quadratic function in ρ_Γ with \mathcal{E}_0 and κ_0 held fixed and the large λ behaviour of ρ_Γ and θ_Γ crucially depend on the sign of κ_0 . Since \mathcal{E}_0^2 is a positive constant and θ_Γ^2 is positive (θ_Γ is real), it follows that if $\kappa_0 < 0$ then ρ_Γ in (34) cannot be arbitrarily large.

$$\text{If } \kappa_0 < 0 \text{ then } \rho_\Gamma \text{ is bounded from above.} \quad (35)$$

However, if $\kappa_0 \geq 0$ then no such bound on ρ_Γ exists and, in principle, ρ_Γ and θ_Γ can attain arbitrarily large values. In fact, as will now be shown, if $\kappa_0 > 0$ then ρ_Γ may diverge in *finite* proper time.

Assume that the initial data satisfies $\kappa_0 > 0$ and $\theta_0 < 0$. Using (34) to eliminate θ_Γ^2 from the right-hand side of (32) leads to

$$\frac{d\theta_\Gamma}{d\lambda} = -\rho_\Gamma - \kappa_0\rho_\Gamma^2 \quad (36)$$

and since $\rho_\Gamma \geq 0$, $\kappa_0 > 0$ and $\theta_0 < 0$ it follows from (36) that $\theta_\Gamma < 0$. Therefore, using the *negative* root of (34),

$$\theta_\Gamma = -\sqrt{\mathcal{E}_0^2 + 2\rho_\Gamma + \kappa_0\rho_\Gamma^2},$$

to eliminate θ_Γ from the right-hand side of (31)

$$\frac{d\rho_\Gamma}{d\lambda} = \rho_\Gamma \sqrt{\mathcal{E}_0^2 + 2\rho_\Gamma + \kappa_0\rho_\Gamma^2}$$

is obtained and ρ_Γ asymptotes at proper time λ_∞ where

$$\lambda_\infty = \int_{\rho_0}^{\infty} \frac{1}{\rho_\Gamma \sqrt{\mathcal{E}_0^2 + 2\rho_\Gamma + \kappa_0 \rho_\Gamma^2}} d\rho_\Gamma. \quad (37)$$

The integrand is positive and $(\mathcal{E}_0^2 + 2\rho_\Gamma) > 0$ so (37) implies

$$\begin{aligned} \lambda_\infty &< \int_{\rho_0}^{\infty} \frac{1}{\rho_\Gamma \sqrt{\kappa_0 \rho_\Gamma^2}} d\rho_\Gamma \\ &= \frac{1}{\rho_0 \sqrt{\kappa_0}} \end{aligned}$$

i.e. λ_∞ is bounded from above.

$$\begin{aligned} \text{If } \kappa_0 > 0 \text{ and } \theta_0 < 0 \text{ at } \lambda = 0 \text{ then } \rho_\Gamma \text{ diverges} \\ \text{at proper time } \lambda = \lambda_\infty \text{ less than } 1/(\rho_0 \sqrt{\kappa_0}). \end{aligned} \quad (38)$$

The constant κ_0 may be obtained in terms of data on the spacelike hypersurface $t = 0 = T(0)$ where (t, z) is the laboratory coordinate system. Let $\mu(0, z)$ be the initial Newtonian velocity measured in the laboratory frame (see (5) for the definition of μ). Using (5), $\theta = \bar{\nabla} \cdot V$ and (7) it follows that

$$\theta = \partial_t \gamma + \partial_z (\gamma \mu), \quad (39)$$

$$\partial_t \gamma + \mu \partial_z \gamma = \mathcal{E} \mu \quad (40)$$

where $\gamma = 1/\sqrt{1 - \mu^2}$. Using (40) to eliminate $\partial_t \gamma$ from (39) yields

$$\theta = \mathcal{E} \mu + \gamma \partial_z \mu$$

and so on the initial spacelike hypersurface $t = 0$

$$\theta_0 = \mathcal{E}_0 \mu_0 + \gamma_0 (\partial_z \mu)_0 \quad (41)$$

where $\mu_0 = (\Gamma^* \mu)(0)$, $(\partial_z \mu)_0 = (\Gamma^* (\partial_z \mu))(0)$. Using (41) to eliminate $\theta_0 = \theta_\Gamma(0)$ in (34) evaluated at $\lambda = 0$ gives

$$\kappa_0 = \frac{1}{\rho_0^2} \left(\gamma_0^2 (\partial_z \mu)_0^2 + 2\mathcal{E}_0 \mu_0 \gamma_0 (\partial_z \mu)_0 - \frac{\mathcal{E}_0^2}{\gamma_0^2} - 2\rho_0 \right). \quad (42)$$

Equation (42) indicates that if $(\partial_z \mu)_0 = 0$ then $\kappa_0 < 0$ and according to (35) ρ_Γ does not diverge. This result agrees with the non-singular behaviour of the exact solutions to (6-8) satisfying $\mu(0, z) = 0$ presented in [3]; for κ_0 to be positive $(\partial_z \mu)_0$ must be non-zero.

The integral curves of V for the particular solution to equations (6-8) with the initial conditions

$$\mathcal{E}(0, z) = \frac{1}{2} \left(\int_{-\infty}^z \frac{\rho(0, s)}{\sqrt{1 - \mu(0, s)^2}} ds - \int_z^{\infty} \frac{\rho(0, s)}{\sqrt{1 - \mu(0, s)^2}} ds \right),$$

$$\rho(0, z) = 0.01 \exp(-z^2),$$

$$\mu(0, z) = 0.1 \sin(z)$$

are shown in figure 1. Trajectories on which $\kappa_0 > 0$ and $\theta_0 < 0$ are solid and trajectories on which $\kappa_0 < 0$ are dashed. Thus, according to (38), ρ diverges at points along the solid trajectories, which meet at about $t = 11$. The details of the onset of the crossings are shown in figure 2 with proper time λ and z as axes. Evaluating (37) gives $\lambda_\infty = 10.14$ for the trajectory starting at $(t, z) = (0, 3)$. Any comoving coordinate system (τ, σ)

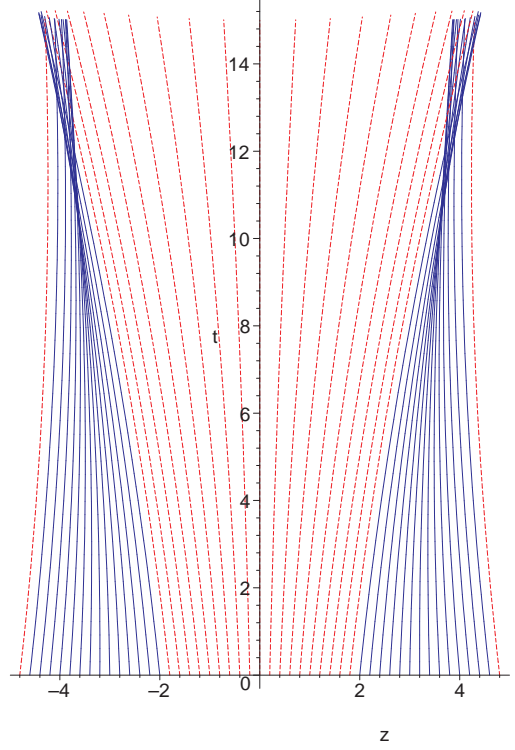


FIG. 1: The integral curves of V for a particular solution to equations (6-8).

adapted to the trajectories, where σ is constant on each trajectory, degenerates where the solid trajectories cross. The determinant of the Jacobian of the $(\tau, \sigma) \rightarrow (t, z)$ transformation vanishes at such points and ρ diverges.

IV. DISCUSSION OF CROSSING TRAJECTORIES IN CHARGED PARTICLE BEAMS

In fluid and gas dynamics, crossing trajectories are considered to be a symptom of incomplete physics. All real fluids and gases are viscous to some extent and trajectories may cross if their viscosity is neglected. For example, a compression wave in a hypothetical inviscid fluid may lead to a velocity field with crossing characteristics, i.e. the velocity becomes multi-valued. In reality this is not what happens; the velocity remains single-valued and stabilises to form a propagating shock. The fluid on either side of the shock is essentially inviscid but close to the

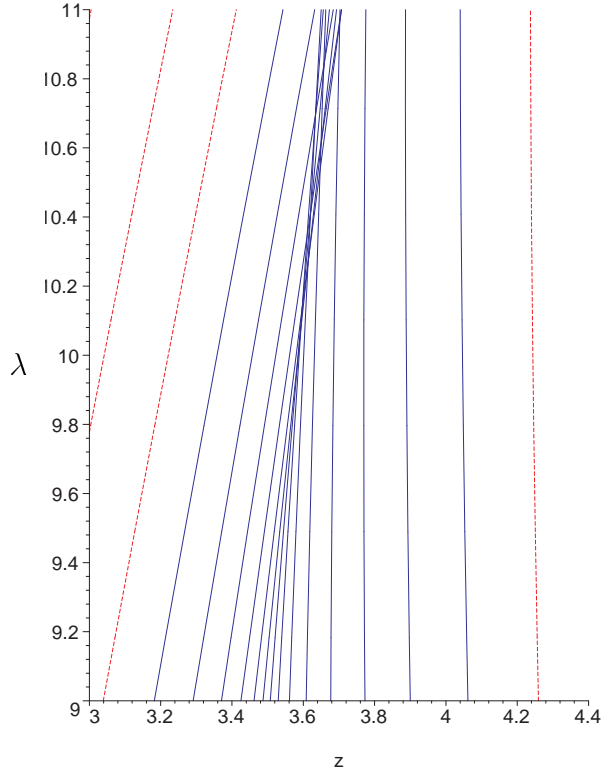


FIG. 2: The integral curves of V for a particular solution to equations (6-8).

shock the second-order spatial derivatives of the velocity are so large that dissipation can no longer be neglected.

However, it is far from clear that such arguments are relevant for a charged particle beam, which is physically very different from a normal fluid. Although (1-4) are often said to describe a “cold charged fluid” [5], this terminology is misleading. Microscopically, a normal fluid is a complicated system of neutral particles whose interactions are dominated by molecular collisions and possibly gravity but the dominant inter-particle forces in a beam of electrons are entirely electromagnetic in origin. At first sight, it seems that all of the necessary physics is contained in (1-4).

The velocity field V is a smoothed out representation of the particle motion. The fact that the trajectories cross does not mean that the particles are colliding; it merely indicates that a smooth field representation of the particles has degenerated. Similarly, the 3-volume number density of a collection of particles may attain arbitrarily large values if the particles dynamically arrange themselves into planar or linear configurations.

Nevertheless, the electric field induced by V in (1-4) is inconsistent where trajectories of V cross. Equation (9) indicates that the electric field in any wall-of-charge solution is constant along V . However, during the crossing the charge distribution “passes through itself” and the electric field has to change. The reason for this is easiest to appreciate by the following simple analogy. Consider

the dynamics of a pair of positive *sheet* charges that are permitted to pass through each other. The sheets are arranged so that their normals and their electric fields lie along the z -axis. Each sheet has the same properties; its self-induced electric field is E at all points to its right and $-E$ at all points to its left, where $E > 0$ is constant, and its charge per unit area is $Q = 2\epsilon_0 E$. The sheets are labelled 1 and 2 and sheet 1 lies to the left of sheet 2 initially. The electrostatic force acting on each sheet is constant and is due to the electric field of the other sheet. The force per unit area acting on sheet 1 is $-QE$ and on sheet 2 is QE . Thus, the sheets will repel each other but their electric forces will not be enough to stop them meeting for sufficiently large opposing initial velocities. Let the initial velocities be so large that the sheets pass through each other. At all times before they meet, the force on sheet 1 is $-QE$ and the force on sheet 2 is QE . After they meet their rôles have been exchanged; sheet 2 is acted on by $-QE$ while sheet 1 is acted on by QE . Now consider a large number of sheets undergoing collective motions in which only *some* of the sheets pass through each other. A continuum realisation of this model is a dynamical set of component continua each with its own velocity field. The number of components evolves in time and depends on the history of the total continuum.

The spacetime fields (V, ρ) satisfying (1-4) offer an Eulerian description of a single component continuum. Although a dynamical number of components can be simulated using more complicated Eulerian field theories [6], such approaches are restrictive because an upper bound must be placed on the number of anticipated components. In the following section a new Lagrangian model of a multi-component charged continuum is proposed in which the number of components is dynamical and free to attain *any* value. The essential idea is to describe the bulk particle motion using a flow map C from a body-time manifold into spacetime rather than inducing the motion from a velocity field V on spacetime. C may be described as “folding” a single electric current on the body-time manifold to give a multi-component current on spacetime.

V. LAGRANGIAN DESCRIPTION OF MULTI-COMPONENT CHARGED CONTINUA

Ingredients in the following Lagrangian description are an auxiliary 4-dimensional manifold \mathcal{B}_4 called the *body-time* manifold and a map C from \mathcal{B}_4 into Minkowski spacetime \mathcal{M}_4 . The body-time manifold $\mathcal{B}_4 = \mathbb{R} \times \mathcal{B}_3$ where \mathcal{B}_3 is a 3-dimensional *body* manifold so each point $P \in \mathcal{B}_4$ is also written $P = (\lambda, \underline{P})$ for $\lambda \in \mathbb{R}$ and $\underline{P} \in \mathcal{B}_3$. Each point $\underline{P} \in \mathcal{B}_3$ generates a curve $C_{\underline{P}}$ in spacetime \mathcal{M}_4 where

$$C_{\underline{P}}(\lambda) = C(\lambda, \underline{P}).$$

The map C is normalised so that λ is the proper-time parameter of $C_{\underline{P}}$ for all $\underline{P} \in \mathcal{B}_3$:

$$g(\dot{C}, \dot{C}) = -1 \quad (43)$$

where $\dot{C}(P) = (C_* \partial_\lambda)(P)$ is a vector at $p = C(P)$ in \mathcal{M}_4 .

In general, C is a many-to-one map, i.e. there exists P_1 and P_2 in \mathcal{B}_4 such that $C(P_1) = C(P_2)$, and C is not required to be surjective. For any point $p \in \mathcal{M}_4$ there may exist any number $N(p)$ of real roots of the equation $p = C(P)$. The map C describes “multi-valued velocities” because although $C(P_1) = C(P_2)$, there is no reason why $\dot{C}(P_1)$ should equal $\dot{C}(P_2)$. Thus, in general \dot{C} cannot be identified with a vector field on \mathcal{M}_4 . The domain of \dot{C} is \mathcal{B}_4 and $\dot{C}(P)$ is a vector at the point $C(P)$; the map \dot{C} is referred to as a vector field over C .

The map C is defined to satisfy the Lorentz force equation

$$\nabla_{\dot{C}} \tilde{C} = i_{\dot{C}} F \quad (44)$$

where F is an electromagnetic field 2-form on \mathcal{M}_4 and $(\nabla_{\dot{C}} \tilde{C})(P)$ and $i_{\dot{C}(P)} F(p)$ are covectors at $p = C(P)$.

The maps $\nabla_{\dot{C}} \tilde{C}$ and $i_{\dot{C}} F$ are covector fields over C (i.e. 1-forms over C).

The set inverse C^{-1} of C at p includes the set of points in \mathcal{B}_4 for which $p = C(P)$ and is written

$$C^{-1}(\{p\}) = \begin{cases} \{P_{[1]}, P_{[2]}, \dots, P_{[N(p)]}\} & \text{if } N(p) \geq 1 \\ \emptyset & \text{if } N(p) = 0 \end{cases}$$

where the square brackets distinguish root labels from coordinate and frame labels.

Each element of $C^{-1}(\{p\})$ gives rise to a *partial* electric 4-current $J_{[i]}(p)$, where $i = 1, 2, \dots, N(p)$. The sum of partial currents is the total electric 4-current driving F in the Maxwell equations

$$dF = 0, \quad (45)$$

$$d \star F = - \sum_{i=0}^{N(p)} \star \widetilde{J}_{[i]}. \quad (46)$$

Regions of spacetime with different numbers of partial currents are distinguished by examining the pull-back $C^*(\star 1)$ of the spacetime volume 4-form $\star 1$ by C . *Critical* points in \mathcal{B}_4 are defined by the vanishing of the 4-form $C^*(\star 1)$. Their images under C are also said to be critical and lie in the interfaces between spacetime regions with different $N(p)$. Specifying a non-vanishing closed 3-form \mathcal{J} on \mathcal{B}_4 satisfying

$$i_{\partial_\lambda} \mathcal{J} = 0, \quad \mathcal{L}_{\partial_\lambda} \mathcal{J} = 0 \quad (47)$$

leads to a scalar field Δ on \mathcal{B}_4 where

$$\Delta d\lambda \wedge \mathcal{J} = C^*(\star 1) \quad (48)$$

which vanishes at critical points. At each point p in \mathcal{M}_4 the partial 4-current $J_{[i]}(p)$ has the form

$$J_{[i]}(p) = \varrho(P_{[i]}) \dot{C}(P_{[i]}) \quad \text{where } P_{[i]} = C_{[i]}^{-1}(p) \quad (49)$$

and ϱ is the scalar field

$$\varrho = \frac{1}{|\Delta|} \quad (50)$$

on \mathcal{B} . The system (43-46) differs significantly from (1-4) because the number $N(p)$ of elements of $C^{-1}(\{p\})$, and therefore the number of partial 4-currents in (46), depends on the spacetime point p . Numerically integrating (43-46) involves computing $N(p)$ at each time step.

VI. MULTI-COMPONENT CHARGE CONFIGURATIONS

Since (1-4) are equivalent to (43-46) when applied to a spacetime region with a single partial current, it follows that solutions to (1-4) and (43-46) agree in such a region. This is illustrated in figures 3 and 4 by collapsing “wall of charge” solutions to (1-4) and (43-46). The ansätze for F and V are

$$\begin{aligned} F &= \mathcal{E}(t, z) dt \wedge dz, \\ V &= \cosh \chi(t, z) \partial_t + \sinh \chi(t, z) \partial_z \end{aligned}$$

and ρ depends only on (t, z) where (t, x, y, z) is an inertial Cartesian coordinate system with

$$g = -dt \otimes dt + dx \otimes dx + dy \otimes dy + dz \otimes dz.$$

Similarly, C and ϱ only depend on (λ, σ^1) where $(\sigma^1, \sigma^2, \sigma^3)$ is a coordinate system on \mathcal{B}_3 . The initial conditions on \mathcal{E} , χ and ρ are

$$\begin{aligned} \mathcal{E}(0, z) &= \frac{1}{2} \left(\int_{-\infty}^z (\rho \cosh \chi)(0, s) ds - \int_z^\infty (\rho \cosh \chi)(0, s) ds \right), \\ \rho(0, z) &= \begin{cases} 0.025 & \text{if } -1.5 \leq z \leq 1.5 \\ 0 & \text{otherwise,} \end{cases} \\ \chi(0, z) &= -1.2 \tanh(z) \end{aligned} \quad (51)$$

with analogous initial conditions on C and ϱ .

In both cases a critical point develops at $p_{\text{crit}} = (0, 1.075)$. The integral curves of V in the single-component Eulerian model (1-4) exhibit crossings along a narrow corridor inside the forward light-cone of p_{crit} (see figure 3). However, the solution to (43-46) shown in figure 4 contains a “fan” of three partial currents inside p_{crit} ’s forward light-cone. The two models clearly yield dramatically different results.

On the other hand, the two models agree outside the forward light-cone at p_{crit} . An argument for this is as follows: Integrate (1-4) and (43-46) using a time slicing adapted to a field of synchronised inertial observers

moving along the z -axis in the laboratory frame with positive constant velocity arbitrarily close to the speed of light. As before, the solutions agree up to a constant proper time surface containing the point p_{crit} . Part of this proper time hypersurface almost coincides with the $z > 0$ subset of p_{crit} 's forward light cone. Now integrate the equations using a time-slicing adapted to a field of synchronised inertial observers moving along the z -axis in the negative direction at almost the speed of light. The result agrees almost up to the $z < 0$ subset of p_{crit} 's forward light-cone. It follows that the solutions to (1-4) and (43-46) agree at points outside the forward light-cone at p_{crit} .

For further comparison the reduced proper charge densities for (1-4) and (43-46) are shown in figures 5 and 6.

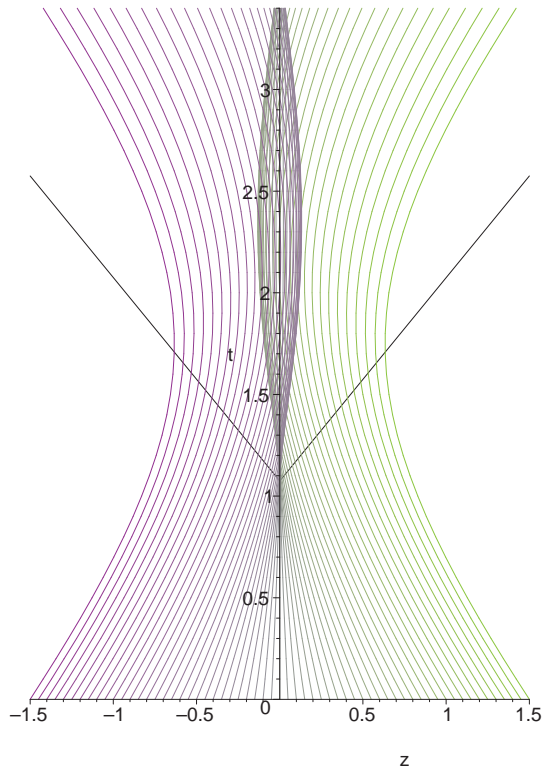


FIG. 3: The trajectories of the particular solution to (1-4) with the initial conditions (51). Trajectories cross in a narrow region inside the forward light-cone of the critical point $p_{\text{crit}} = (0, 1.075)$.

VII. ULTRA-RELATIVISTIC APPROXIMATION SCHEME

Ultra-relativistic solutions to (1-4) may be obtained by promoting (V, ρ, F) to a 1-parameter family $(V^\varepsilon, \rho^\varepsilon, F^\varepsilon)$ in ε where the ε dependences are motivated by exact “wall of charge” solutions [3]. The equations obtained

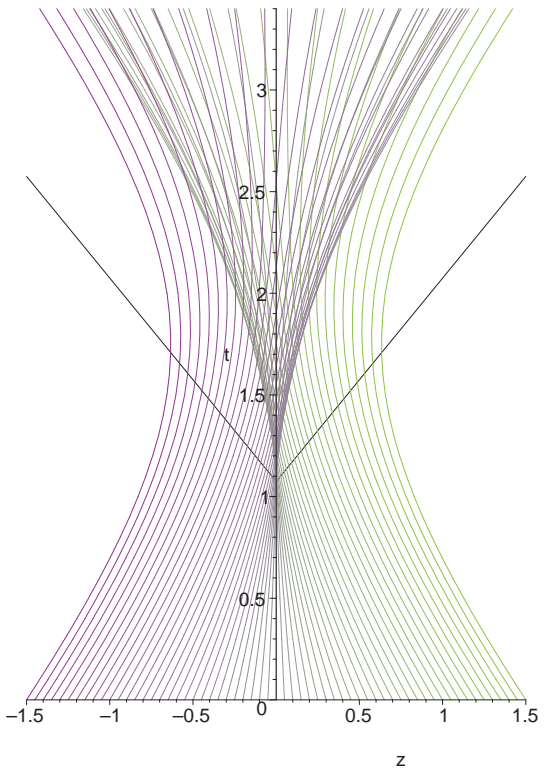


FIG. 4: The trajectories of the particular solution to (43-46) with the initial conditions (51). The forward light-cone of the critical point $p_{\text{crit}} = (0, 1.075)$ is also shown. The region outside the “fan” emanating from p_{crit} has only one partial current whereas the region inside the “fan” contains three partial currents.

by equating orders in ε lead to a self-consistent hierarchical method for approximating solutions to (1-4). The virtue of the scheme is that the ε dependences conspire to produce an infinite tower of equations that are partially coupled and are generally easier to solve than the fully coupled system (1-4).

A similar approach based on (43-46) will now be outlined. Let C^ε be a 1-parameter family of maps from \mathcal{B}_4 into \mathcal{M}_4 such that

$$g(\dot{C}^\varepsilon, \dot{C}^\varepsilon) = -1$$

where $\dot{C}^\varepsilon = C_*^\varepsilon \partial_\lambda$. Let $\lambda = \varepsilon s$ and introduce the map \mathcal{C}^ε where

$$\mathcal{C}^\varepsilon(s, \underline{P}) = C^\varepsilon(\varepsilon s, \underline{P}) \quad (52)$$

at all non-critical points in the domain of C^ε . Thus

$$\dot{C}^\varepsilon = \frac{1}{\varepsilon} \mathcal{C}_*^\varepsilon \partial_s = \frac{1}{\varepsilon} \mathcal{C}^{\varepsilon'} \quad (53)$$

where $\mathcal{C}^{\varepsilon'} = \mathcal{C}_*^\varepsilon \partial_s$ and so

$$g(\mathcal{C}^{\varepsilon'}, \mathcal{C}^{\varepsilon'}) = -\varepsilon^2. \quad (54)$$

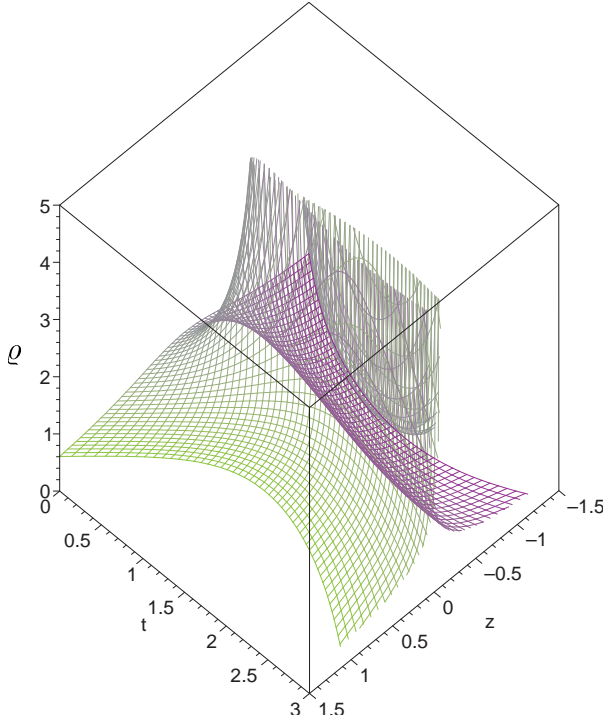


FIG. 5: The reduced proper charge density of the particular solution to (1-4) with the initial conditions (51).

and the Lorentz force equation for \mathcal{C}^ε becomes

$$\nabla_{\mathcal{C}^\varepsilon} \widetilde{\mathcal{C}^\varepsilon} = \varepsilon i_{\mathcal{C}^\varepsilon} F^\varepsilon. \quad (55)$$

In [3] a dependence for V^ε on ε of the form

$$V^\varepsilon = \sum_{n=1}^{\infty} \varepsilon^n V_n \quad (56)$$

was motivated by ‘‘wall of charge’’ solutions to (1-4). For multi-current configurations on Minkowski spacetime \mathcal{M}_4 , the flow map \mathcal{C} is the dependent variable and it is natural to exploit the affine structure of \mathcal{M}_4 and postulate an analogous series for \mathcal{C}^ε . Let (x^a) be an inertial Cartesian coordinate system adapted to the laboratory frame on \mathcal{M}_4 where $a, b = 0, 1, 2, 3$ and

$$g = \eta_{ab} dx^a \otimes dx^b$$

where

$$\eta_{ab} = \begin{cases} -1 & \text{if } a = b = 0 \\ 1 & \text{if } a = b \neq 0 \\ 0 & \text{if } a \neq b. \end{cases}$$

In the rest of this article the map \mathcal{C}^ε is also regarded as the 4-component column vector

$$\begin{pmatrix} \mathcal{C}^{\varepsilon 0} \\ \mathcal{C}^{\varepsilon 1} \\ \mathcal{C}^{\varepsilon 2} \\ \mathcal{C}^{\varepsilon 3} \end{pmatrix}$$

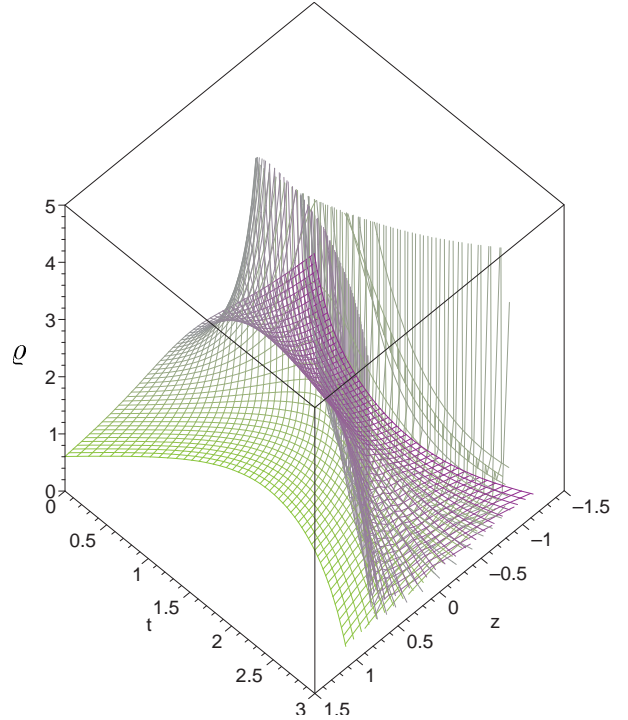


FIG. 6: The partial reduced proper charge densities of the particular solution to (43-46) with the initial conditions (51). The region outside the ‘‘fan’’ has only one partial current whereas the region inside the ‘‘fan’’ contains three partial currents.

where $(\mathcal{C}^{\varepsilon a})$ are the (x^a) components of \mathcal{C}^ε .

The ε expansions of $\mathcal{C}^{\varepsilon a}(Q)$, where $Q = (s, \underline{P})$, are chosen as

$$\mathcal{C}^{\varepsilon a}(Q) = \sum_{n=0}^{\infty} \varepsilon^n \mathcal{C}_n^a(Q). \quad (57)$$

Motivated by the corresponding expression in the Eulerian single-current formulation [3], the 1-parameter family F^ε of electromagnetic 2-forms is chosen as

$$F^\varepsilon(p) = \sum_{n=-1}^{\infty} \varepsilon^n F_n(p) \quad (58)$$

at any point p in \mathcal{M}_4 . Note that (58) is independent of the ε expansion of \mathcal{C}^ε in (57); F^ε is a 1-parameter family of 2-forms on Minkowski spacetime \mathcal{M}_4 and (58) is *not* the ε expansion of the 2-form $F^\varepsilon(\mathcal{C}^\varepsilon(Q))$ on \mathcal{B}_4 .

One way to minimise the complexity of the ensuing calculation is to adapt a coordinate system on \mathcal{B}_3 to \mathcal{J} . Let (ξ^1, ξ^2, ξ^3) be a coordinate system on \mathcal{B}_3 and let \mathcal{J}_{123} be the corresponding component of \mathcal{J} :

$$\mathcal{J} = \mathcal{J}_{123} d\xi^1 \wedge d\xi^2 \wedge d\xi^3. \quad (59)$$

Eliminating ρ in $J_{[i]}$ in favour of \mathcal{J} and C using (48-50) and (59) yields

$$J_{[i]}(p) = \left| \frac{\mathcal{J}_{123}(P_{[i]})}{\det(\mathbf{D}C)(P_{[i]})} \right| \dot{C}(P_{[i]})$$

where $P_{[i]} = C_{[i]}^{-1}(p) = (\lambda, \xi^1, \xi^2, \xi^3)$ and \mathbf{DC} is the Jacobian of $C^a(\lambda, \xi^1, \xi^2, \xi^3)$. By definition, \mathcal{J}_{123} is independent of λ (see (47)) so (ξ^1, ξ^2, ξ^3) may be chosen so that $|\mathcal{J}_{123}| = 1$. Hence

$$\begin{aligned} J_{[i]}(p) &= \frac{1}{|\det(\mathbf{DC})(P_{[i]})|} \dot{C}(P_{[i]}) \\ &= \frac{1}{|(\det(\mathbf{DC}) \circ C_{[i]}^{-1})(p)|} (\dot{C} \circ C_{[i]}^{-1})(p) \end{aligned}$$

and so

$$J_{[i]}^{\varepsilon a}(p) = \frac{1}{|(\det(\mathbf{DC}^\varepsilon) \circ \mathcal{C}_{[i]}^{\varepsilon-1})(p)|} (\mathcal{C}^{\varepsilon'} \circ \mathcal{C}_{[i]}^{\varepsilon-1})^a(p) \quad (60)$$

where (52) and (53) have been used, \mathbf{DC}^ε is the Jacobian of $\mathcal{C}^{\varepsilon a}(s, \xi^1, \xi^2, \xi^3)$ and $\mathbf{DC}^\varepsilon = \frac{1}{\varepsilon} \mathbf{DC}^\varepsilon$.

Let $F_b^{\varepsilon a} = \eta^{ac} F_{bc}^\varepsilon$ where $F^\varepsilon = \frac{1}{2} F_{ab}^\varepsilon dx^a \wedge dx^b$ and $\eta^{ac} \eta_{cb} = \delta_b^a$ where

$$\delta_b^a = \begin{cases} 1 & \text{if } a = b \\ 0 & \text{if } a \neq b. \end{cases}$$

The inertial coordinate representations of the Lorentz force equation (55) for \mathcal{C}^ε and the normalisation constraint (54) are

$$\mathcal{C}^{\varepsilon a''} = \varepsilon (F_b^{\varepsilon a} \circ \mathcal{C}^\varepsilon) \mathcal{C}^{\varepsilon b'}, \quad \eta_{ab} \mathcal{C}^{\varepsilon a'} \mathcal{C}^{\varepsilon b'} = -\varepsilon^2 \quad (61)$$

where F^ε is a solution to the Maxwell equations

$$dF^\varepsilon = 0, \quad d \star F^\varepsilon = - \sum_{i=0}^{N(p)} \star \widetilde{J}_{[i]}^\varepsilon \quad (62)$$

and $J_{[i]}^\varepsilon$ is given in (60).

Inserting (57) and (58) into (61) and (62) and equating equal order terms in ε induces a hierarchy of equations for successive approximations to $(\mathcal{C}^\varepsilon, F^\varepsilon)$. The first six steps in the hierarchy are:

- Adopt an external electromagnetic field F_{-1} , i.e. a solution to the source-free Maxwell equations

$$dF_{-1} = 0, \quad d \star F_{-1} = 0.$$

- Solve

$$\mathcal{C}_0^{a''}(Q) = (F_{-1})_b^a(p) \mathcal{C}_0^{b'}(Q)$$

for \mathcal{C}_0^a subject to

$$\eta_{ab} \mathcal{C}_0^{a'}(Q) \mathcal{C}_0^{b'}(Q) = 0$$

where $p = \mathcal{C}_0(Q)$ and $(F_{-1})_b^a$ is data obtained in the previous step.

- The 2-form F_0 is a solution to the Maxwell equations

$$dF_0 = 0, \quad d \star F_0 = - \sum_{i=0}^{N(p)} \star \widetilde{J}_{[i]0}$$

and

$$J_{[i]0}^a(p) = |\det(\mathbf{DC}_{[i]0}^{-1})(p)| \mathcal{C}_{[i]0}^{a'}(Q) \quad (63)$$

where $\mathbf{DC}_{[i]0}^{-1}(p)$ is the Jacobian of $\mathcal{C}_{[i]0}^{-1}$ at $p = (x^a)$ and $Q = \mathcal{C}_{[i]0}^{-1}(p)$.

- The first order correction \mathcal{C}_1 to the map \mathcal{C}_0 is obtained from the linear equation

$$\mathcal{C}_1^{a''} = (F_{-1})_b^a \mathcal{C}_1^{b'} + (F_{-1})_b^a, c \mathcal{C}_1^c \mathcal{C}_0^{b'} + (F_0)_b^a \mathcal{C}_0^{b'}$$

subject to

$$\eta_{ab} \mathcal{C}_0^{a'} \mathcal{C}_1^{b'} = 0$$

where maps on \mathcal{B}_4 are implicitly evaluated at Q and maps on \mathcal{M}_4 are evaluated at $p = \mathcal{C}_0(Q)$. Indices following a comma indicate partial differentiation with respect to the corresponding coordinates so $(F_{-1})_b^a, c = \frac{\partial}{\partial x^c} (F_{-1})_b^a$.

- The 2-form F_1 is a solution to the Maxwell equations

$$dF_1 = 0, \quad d \star F_1 = - \sum_{i=0}^{N(p)} \star \widetilde{J}_{[i]1}$$

and

$$\begin{aligned} J_{[i]1}^a = & |\det(\mathbf{DC}_{[i]0}^{-1})| \left[-\text{tr}(\mathbf{DC}_{[i]0}^{-1} \mathbf{DC}_1) \mathcal{C}_0' \right. \\ & + \left\{ \text{tr}(\mathbf{DC}_{[i]0}^{-1} \mathbf{D}^2 \mathcal{C}_0)^T \mathbf{DC}_{[i]0}^{-1} \mathcal{C}_1 \right\} \mathcal{C}_0' \\ & \left. + \mathcal{C}_1' - \mathbf{DC}_0' \mathbf{DC}_{[i]0}^{-1} \mathcal{C}_1 \right] \end{aligned}$$

where maps on \mathcal{M}_4 are implicitly evaluated at p and maps on \mathcal{B}_4 are implicitly evaluated at $Q = \mathcal{C}_{[i]0}^{-1}(p)$. Inside the square brackets \mathbf{DC}_1 is the matrix of derivatives of \mathcal{C}_1^a and \mathbf{DC}_0' is the matrix of derivatives of \mathcal{C}_0^a and both should be regarded as linear maps from the $(\xi^0 = \lambda, \xi^1, \xi^2, \xi^3)$ components of vectors on \mathcal{B}_4 to the (x^a) components of vectors on \mathcal{M}_4 . Similarly, inside the square brackets $\mathbf{DC}_{[i]0}^{-1}$ should be regarded as a linear mapping from the (x^a) components of vectors on \mathcal{M}_4 to the (ξ^a) components of vectors on \mathcal{B}_4 . The column vector $\text{tr}(\mathbf{DC}_{[i]0}^{-1} \mathbf{D}^2 \mathcal{C}_0)$ is

$$\begin{pmatrix} \text{tr}(\mathbf{DC}_{[i]0}^{-1} \mathbf{D} \partial_\lambda \mathcal{C}_0) \\ \text{tr}(\mathbf{DC}_{[i]0}^{-1} \mathbf{D} \partial_{\xi^1} \mathcal{C}_0) \\ \text{tr}(\mathbf{DC}_{[i]0}^{-1} \mathbf{D} \partial_{\xi^2} \mathcal{C}_0) \\ \text{tr}(\mathbf{DC}_{[i]0}^{-1} \mathbf{D} \partial_{\xi^3} \mathcal{C}_0) \end{pmatrix}$$

where $\mathbf{D} \partial_\zeta \mathcal{C}_0$ is the matrix of partial derivatives of $\partial_\zeta \mathcal{C}_0$ where $\zeta = \lambda, \xi^1, \xi^2, \xi^3$.

- The second order correction \mathcal{C}_2 to \mathcal{C} is a solution to the equation

$$\begin{aligned}\mathcal{C}_2^{a''}(Q) &= (F_{-1})_b{}^a \mathcal{C}_2^{b'} + (F_{-1})_b{}^a,{}_c \mathcal{C}_1^c \mathcal{C}_1^{b'} \\ &+ \frac{1}{2} (F_{-1})_b{}^a,{}_{cd} \mathcal{C}_1^c \mathcal{C}_1^d \mathcal{C}_0^{b'} + (F_{-1})_b{}^a,{}_c \mathcal{C}_2^c \mathcal{C}_0^{b'} \\ &+ (F_0)_b{}^a \mathcal{C}_1^{b'} + (F_0)_b{}^a,{}_c \mathcal{C}_1^c \mathcal{C}_0^{b'} + (F_1)_b{}^a \mathcal{C}_0^{b'}\end{aligned}$$

subject to

$$2\eta_{ab} \mathcal{C}_0^{a'} \mathcal{C}_2^{b'} + \eta_{ab} \mathcal{C}_1^{a'} \mathcal{C}_1^{b'} = -1$$

where $p = \mathcal{C}_0(Q)$.

Note that \mathcal{C}_0' and $\mathcal{C}_0' + \varepsilon \mathcal{C}_1'$ are lightlike and $\mathcal{C}_0' + \varepsilon \mathcal{C}_1' + \varepsilon^2 \mathcal{C}_2'$ is the leading order timelike approximation to \mathcal{C}^ε .

In single-current regions the reduced proper charge density is $\sqrt{-g(J_{[1]}^\varepsilon, J_{[1]}^\varepsilon)}$ on spacetime. Using (57), (60) and the normalisation condition (61) on \mathcal{C}^ε it follows that $\sqrt{-g(J_{[1]}^\varepsilon, J_{[1]}^\varepsilon)}$ converges to 0 as ε tends to 0. The reduced proper charge density diverges on interfaces between single-current and multi-current regions and the above approximation scheme is valid arbitrarily close to such interfaces.

VIII. CONCLUSION

Continuum models of charged particle beams include the interaction of matter with its own electromagnetic field and avoid peculiar phenomena evident in point-particle descriptions of self-interacting charge, such as self-acceleration and pre-acceleration. A field-theoretic realisation of a collection of classical electrons is the “cold” charged continuum. It was shown that the velocity field of the continuum may possess crossing trajectories and in this case the Eulerian theory is inconsistent. Such behaviour is not uncommon in physics; compression waves in inviscid fluids also develop crossing trajectories. However, inviscid fluids are an idealisation; all

normal fluids are viscous to some extent and ameliorate the problem by forming a shock. On the other hand, a beam of electrons is very different from a normal fluid and it was argued that there is no physical reason why the trajectories modelling an electron beam cannot cross. A Lagrangian theory permitting crossing trajectories was presented and its “wall of charge” solutions were examined and compared with solutions to the original Eulerian field system. Finally, an approximation scheme was developed to analyse ultra-relativistic charge configurations of the Lagrangian system.

The Lagrangian theory discussed here features an N -component electric current where N is dynamically determined and has a point-wise dependence on spacetime. It is possible that configurations with $N = 1$ initially may evolve into highly complicated “turbulent” configurations where N is arbitrarily large. Further work in this context may be found in [7].

The theory developed here has immediate application to high-energy accelerator physics where ultra-relativistic motion is ubiquitous. The general approach is also valid in systems where electromagnetic interactions dominate over collisional processes, such as in laser-driven plasma wakefield accelerators where the transition between single and multiple component electron currents (“wave breaking”) [8] has recently received much attention.

Acknowledgments

The authors are grateful to the Cockcroft Institute for making this work possible, to EPSRC for a Portfolio award and to the EC for a Framework 6 (FP6-2003-NEST-A) award. RWT is also grateful to EPSRC for a Springboard Fellowship.

[1] P.A.M. Dirac, Proc. R. Soc. Lond. **A** 167 148–168 (1938).
[2] L.D. Landau, E.M. Lifshitz, “The Classical Theory of Fields”, Pergamon, Oxford (1962).
[3] D.A. Burton, J. Gratus, R.W. Tucker. Ann. Phys. (in press, available on-line at <http://www.elsevier.com>).
D.A. Burton, J. Gratus, R.W. Tucker. Proceedings of EPAC 2006.
[4] For an introduction to exterior calculus and its application to electromagnetism see, for example, I.M. Benn, R.W. Tucker, “An Introduction to Spinors and Geometry with Applications in Physics”, Adam Hilger (1987).
[5] R.C. Davidson, H. Qin, “Physics of intense charged particle beams in high energy accelerators”, World Scientific (2001).
[6] X. Li, J.G. Wöhlbier, S. Jin, J.H. Booske, Phys. Rev. **E** 70, 016502 1–12 (2004).
[7] J. Gratus, D.A. Burton, R.W. Tucker. Proceedings of Conference on Global Integrability and Field Theory, Cockcroft Institute (2006) (to appear).
[8] S.P.D. Mangles, et al, Nature 431 (2004) 535–8,
C.G.R. Geddes, et al, Nature 431 (2004) 538–41,
J. Faure J, et al, Nature 431 (2004) 541–4.
[9] The Einstein summation convention is followed i.e. repeated indices are implicitly summed.